J|A|C|S
ARTICLES
Published on Web 09/24/2004

Self-Assembly of Biocidal Nanotubes from a Single-Chain Diacetylene Amine Salt

Sang Beom Lee,[†] Richard Koepsel,[‡] Donna B. Stolz,[§] Heidi E. Warriner,[||] and Alan J. Russell*,[⊥]

Contribution from the Department of Surgery, McGowan Institute for Regenerative Medicine, Suite 200, 100 Technology Drive, Pittsburgh, Pennsylvania 15219, and Department of Bioengineering, Center for Biologic Imaging, Department of Chemical and Petroleum Engineering, and Department of Chemistry, University of Pittsburgh, Pittsburgh, Pennsylvania 15260

Received March 17, 2004; E-mail: russellaj@upmc.edu

Abstract: We describe the facile two-step synthesis of nanotubes that form pure, well-defined, nanostructured materials. We have synthesized a secondary amine HBr salt as the headgroup of a single-chain diacetylenic lipid. This molecule can form a number of different self-assembled nanostructures in aqueous or organic solvents. In water, this lipid forms a monodisperse preparation of nanotubes at high yields. Partially dissolving a preparation of nanotubes dried from aqueous solution results in a remarkably organized structure that resembles a nanocarpet. Details of the nanotube structure were investigated by scanning electron microscopy, transmission electron microscopy, and small-angle X-ray spectroscopy. The aqueous nanotubes have a cross-sectional diameter of 89 nm. The walls of the tubes are an exquisitely uniform 27 nm thick and are shown to consist of five lipid bilayers with a repeat spacing of 57.8 Å. The chemical structure of the material shows no chiral centers, but suspensions of the nanotubes in an aqueous medium show an unexpected circular dichroism signal. The versatility of this new material as a platform for nanostructure design and synthesis is enhanced by its biocidal activity. This antimicrobial activity along with the regularity the nanostructures will enhance the development of a range of applications from biosensors to artificial retinas.

Introduction

The discovery that complex chiral diacetylene derivatives can self-assemble into nanostructures[1] has led to a search for simpler molecules that retain that activity. This search for novel materials is complicated because the factors governing self-assembly are complex and until a simple system is identified the underlying mechanisms will be difficult to discover.[2−5] Unlike spherical liposomes, lipid tubules are thought to require chiral molecules in their formation and are expected to reflect the chiral nature of the lipids used. This chirality in molecular packing is reflected in helical markings often visible in electron micrographs of tubules and in large peaks observed in their circular dichroism spectra, both of which change handedness when the opposite enantiomer lipid is used.[6] Lack of chirality does not in and of itself prevent self-organization since both chiral and achiral diacetylenic amphiphiles have been shown to form cylindrical microstructures from aqueous solution under quite specific conditions.[7−9] The majority of work, however, has been concentrated on relatively complex chiral, multichain lipids as precursors for microstructured materials.

Earlier studies have shown that, in certain instances, chiral double-chain glycerol-based phosphatidylcholines can exhibit helical and tubular supramolecular morphologies.[2] Unfortunately, the complexity of these molecules makes it difficult to understand whether headgroup size and charge, linkage to a glycerol backbone, hydrophobic tail length, chain terminus, or chirality dominates in the nanostructure self-assembly process. If one could identify a simple, single-chain, diacytelylenic lipid that undergoes self-assembly into a completely uniform nanostructure, the potential for rational design and prediction of self-assembly would be significantly enhanced.

[†] Department of Bioengineering, University of Pittsburgh.
[‡] Department of Chemical and Petroleum Engineering, University of Pittsburgh.
[§] Center for Biologic Imaging, University of Pittsburgh.
[||] Department of Chemistry, University of Pittsburgh.
[⊥] McGowan Institute for Regenerative Medicine.

(1) Yager, P.; Schoen, P. E. *Mol. Cryst. Liq. Cryst.* **1984**, *106*, 371−381.
(2) Schnur, J. M. *Science* **1993**, *262*, 1669−1676.
(3) Thomas, B. N.; Safinya, C. R.; Plano, R. J.; Clark, N. A. *Science* **1995**, *267*, 1635−1638.
(4) Singh, A.; Wong, E. M.; Schnur, J. M. *Langmuir* **2003**, *19*, 1888−1898.
(5) Selinger, J. V.; Spector, M. S.; Schnur, J. M. *J. Phys. Chem. B* **2001**, *105*, 7157−7169.
(6) Thomas, B. N.; Corcoran, R. C.; Cotant, C. L.; Lindemann, C. M.; Kirsch, J. E.; Persichini, P. J. *J. Am. Chem. Soc.* **1998**, *120*, 12178−12186.
(7) Singh, A.; Schoen, P. E.; Schnur, J. M. *J. Chem. Soc., Chem. Commun.* **1988**, 1222.
(8) Lindsell, W. E.; Preston, P. N.; Seddon, J. M.; Rosair, G. M.; Woodman, T. A. J. *Chem. Mater.* **2000**, *12*, 1572−1576.
(9) Pakhomov, S.; Hammer, R. P.; Mishra, B. K.; Thomas, B. N. *Proc. Natl. Acad. Sci. U.S.A.* **2003**, *100*, 3040−3042.

10.1021/ja048463i CCC: $27.50

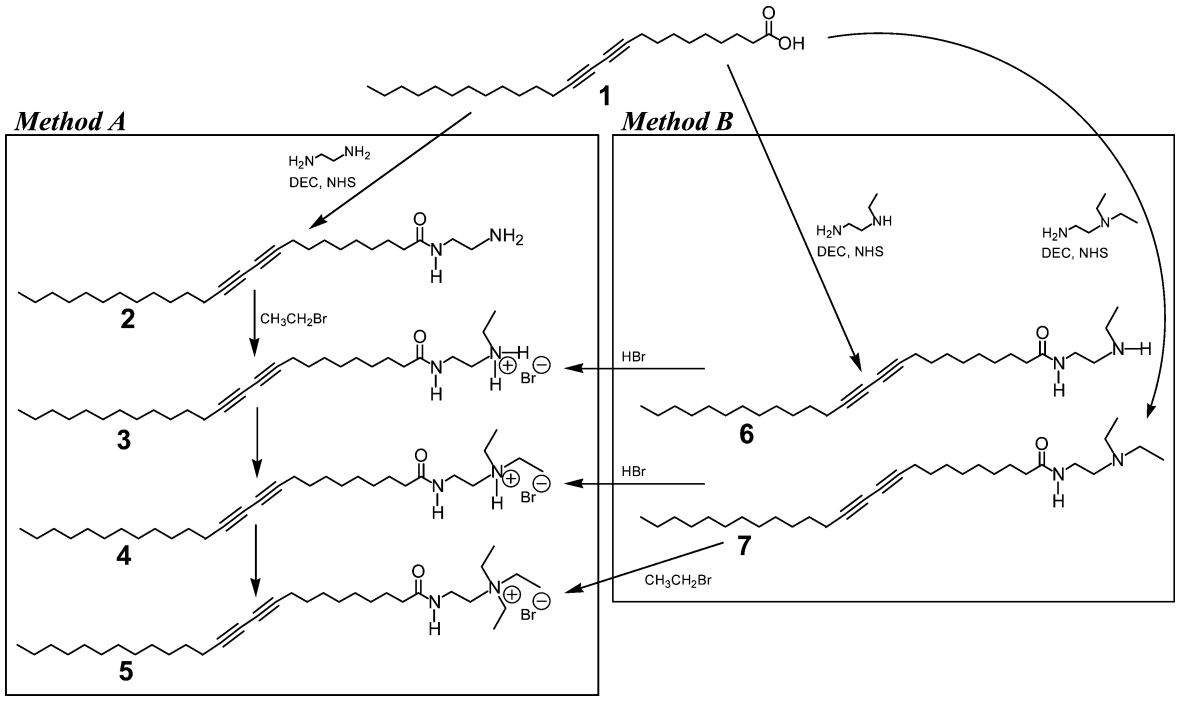

Figure 1. Synthetic strategy.

The simple hydrazide derivatives of single-chain diacetylene lipids described by Jonas et al.[10] show unusual aggregation and polymerization behaviors. Most strikingly, UV cross-linked diacetylenes display a reversible blue/red color change depending on the pH of the surrounding aqueous solution. Specific hydrogen-bonding of the hydrazide groups in balance with hydrophobic interactions in the alkyl tails is found to be responsible for these unusual properties, implying that secondary forces other than chirality can induce the formation of diverse nanostructures.

As an outgrowth of our work to develop materials that both sense and decontaminate chemical and biological weapons,[11−15] we have been searching for nanostructured materials that can kill cells and have the potential to change color while doing so. Some cationic lipids have been shown to exhibit antibacterial activity.[16,17] Further, structure−activity relationships have demonstrated that quaternary ammonium salts cause cell death by disrupting cell membranes and allowing release of the intracellular contents.[18] We had hoped that by synthesizing a cationic lipid with a long-chain diacetylene tail and a quaternary ammonium salt headgroup we would have a molecule capable of acting as both an antimicrobial and a biosensor. We therefore attempted to synthesize the quaternary ammonium salt by direct quaternization of the diacetylene amine compound **2** (Figure 1). The reaction product was found to be a remarkably versatile nanostructure-forming moiety that when self-assembled could kill cells and induce a visible color change. Surprisingly, a detailed analysis of the reaction product revealed a family of amine salt derivatives. Synthesis of seven individual amine, amine salt, and quaternary ammonium salt derivatives of diacetylene demonstrates that the only precursor that has the potential to form nanotubes (in a single step and with 100% yield) is the secondary amine salt (compound **3**). To our knowledge the remarkable self-assembly of this inexpensive and simple lipid is unprecedented and represents a real step toward the rational design of bioactive monodisperse nanostructures.

Materials and Methods

Materials. 10,12-Pentacosadiynoic acid (PDA) was purchased from Fluka. *N*-Hydroxysuccinimide (NHS), 1-[3-(dimethylamino)propyl]-3-ethylcarbodiimide (DEC), ethylenediamine, *N*-ethylethylenediamine, *N*,*N*-diethylethylenediamine, and ethyl bromide were purchased from Aldrich. All organic solvents for synthesis and purification were purchased from Aldrich as reagent grade and were used without further purification.

Synthesis of Diacetylenic Amine Salts. Method A. PDA modified with NHS in the presence of DEC was slowly added to a 10-fold excess of ethylenediamine in dichloroethane. After the reaction, the mixture was washed with water. The organic phase was dried with sodium sulfate and rotary evaporated to yield a white powder. A quaternization reaction was performed by reacting the powdered compound **2** with ethyl bromide in chloroform/nitromethane (1:1) at room temperature for 24 h. Reaction solvents were removed by rotary evaporation, and the resulting white solid was dissolved in a small amount of chloroform followed by slow addition of hexane and drying in a vacuum oven at room temperature.

Method B. PDA modified with NHS in the presence of DEC was slowly added to 10 times excess of *N*-ethylethylenediamine or *N*,*N*-diethylethylenediamine in dichloroethane. After the reaction, the mixture was washed with water. The organic phase was dried with sodium sulfate and rotary evaporated to yield a white powder. Pure compound

(10) Jonas, U.; Shah, K.; Norvez, S.; Charych, D. H. *J. Am. Chem. Soc.* **1999**, *121*, 4580−4588.
(11) Drevon, G. F.; Russell, A. J. *Biomacromolecules* **2000**, *1*, 571−576.
(12) Drevon, G. F.; Hartleib, J.; Scharff, E.; Ruterjans, H.; Russell, A. J. *Biomacromolecules* **2001**, *2*, 664−671.
(13) LeJeune, K. E.; Mesiano, A. J.; Bower, S. B.; Grimsley, J. K.; Wild J. R.; Russell, A. J. *Biotechnol. Bioeng.* **1997**, *54*, 105−114.
(14) Drevon, G. F.; Danielmeier, K.; Federspiel, W.; Stolz, D. B.; Wicks, D. A.; Yu, P. C.; Russell, A. J. *Biotechnol. Bioeng.* **2002**, *79*, 785−794.
(15) Koepsel, R. R.; Russell, A. J. *Biomacromolecules* **2003**, *4*, 850−855.
(16) Tomlinson, E.; Brown, M. R.; Davis, S. S. *J. Med. Chem.* **1977**, *20*, 1277−1282.
(17) McDonnell, G., Russell, A. D. *Clin. Microbiol. Rev.* **1999**, *12*, 147−179.
(18) Merianos, J. J. In *Disinfection, Sterilization, and Preservation*; Block, S. S., Ed.; Lippencott Williams & Wilkins: Philadelphia, 2001; pp 283−320.

3 was prepared from compound **6**. Compound **6** was dissolved in chloroform, and an equal volume of aqueous HBr was added. The mixture was shaken vigorously to transfer the HBr to the organic phase. The organic phase was removed and concentrated in a rotary evaporator. Hexane was added to the chloroform solution to precipitate compound **3**, and the precipitate was dried in vacuo at room temperature.

Nanotube and Nanocarpet Formation. For nanotube formation, 1 mg of the dried reaction products was suspended in 20 mL of water and sonicated for 5 min at 25 °C in a sonic water bath. The solution was transferred onto plain glass slides and dried for 3 h at room temperature. For nanocarpet formation, the above unpolymerized solution was again transferred onto plain glass (25 × 25 mm) slides and dried for 1 h at room temperature. Before the slides were completely dry, one drop of chloroform was added to the surface of the slide and then allowed to dry for 2 h. The process is exquisitely sensitive to initial concentrations of solvent and non-solvent.

Instrumental Analysis. (a) Scanning Electron Microscopy (SEM). Samples were dried onto glass coverslips and then sputter coated with a 3.5 nm coating of gold/palladium (Cressington Auto 108, Cressington, Watford, U.K.). Samples were viewed in a JEOL JEM-6335F scanning electron microscope (JEOL, Peabody, MA) at 5 or 10 kV.

(b) Transmission Electron Microscopy (TEM). Copper grids (200 mesh) were coated using 0.125% Formvar in chloroform and floated on a drop of sample for approximately 30 s. The grids were removed and excess sample solution wicked away with filter paper. The grids were then placed on drops of 0.45 μm filtered 2% phosphotungstic acid, pH 6.0, in Milli-Q H_2O for 30−60 s. Excess stain was wicked away, and the samples were viewed on a JEOL JEM 1210 transmission electron microscope (Peabody, MA) at 80 kV. Samples adhered to coated grids were also viewed without prior staining.

(c) Small-Angle X-ray Scattering (SAXS). SAXS was performed with a Bruker NanoSTAR, consisting of a 6.0 kW rotating anode X-ray generator and area detector with cross-coupled Göbel mirrors for Cu Kα radiation (λ = 1.54 Å). The mirrors produce an approximately parallel beam of about 0.09 mm^2 at the sample position. A Siemens multiwire-type area detector was used. The sample−detector distance was 65.25 cm. Nanotubes in an aqueous solution of 1 or 5 mg/mL concentration were loaded into standard 1.5 mm diameter quartz diffraction capillaries which were flame sealed.

(d) Circular Dichroism (CD). The nanotubes were prepared by dissolving **3** in water at 25 °C at 0.25 mg/mL. The CD studies were performed on a Jasco J-720 spectropolarimeter operating between 175 and 700 nm. The samples were placed in a water-jacketed quartz cell with a path length of 1.0 mm.

Bacterial Methods. (a) Biocidal Assay. To test the biocidal activity of the nanotubes, liquid cultures of *Escherichia coli* K12 were grown overnight in Luria broth. The overnight cultures were diluted in 0.3 mM potassium phosphate (pH 7.2) such that the final concentration of cells was (3−6) × 10^5 cells/mL and used for antimicrobial assays. For the antimicrobial assay 1 mL of a cell suspension was mixed with 1 mL of a 2−20 μg/mL solution of either polymerized or nonpolymerized nanotubes. The mixture was shaken at 37 °C for 1 h, at which time samples were serially diluted and plated on Luria-agar plates. The number of colonies that resulted from overnight incubation of these plates is a direct measure of the number of surviving cells.

(b) Spectrophotmetric Assays. Scanning spectrophotometric assays were used to demonstrate a color change of the polymerized nanotubes upon exposure to bacteria. Bacterial cells, grown as above, were centrifuged and washed three times with distilled water, resuspended in distilled water, diluted to various concentrations, and mixed with nanotubes such that the final concentration of nanotubes was 50 μg/mL. The mixture was immediately placed in a Perkin-Elmer Lambda 45 spectrophotometer and the optical density (OD) measured between 366 and 750 nm. All OD scans were blanked against cells in distilled water.

(c) Electron Microscopy. Transmission electron microscopy to look at the interaction between nanotubes and bacteria was performed essentially as described above except that 1 mL of 10^8 cells/mL was mixed with 1 mL of 100 μg/mL nonpolymerized nanotubes and immediately placed on the microscope grid.

Results and Discussion

Nanotube Formation. Our initial goal was to synthesize compound **5** in an attempt to develop a cell-disrupting material that was also a chemically integrated biosensor. Initial experiments demonstrated that the reaction product from the method A synthesis (Figure 1) had unexpectedly low solubility in water. The reaction product would not be expected to form nanostructures in solution since, until this work, achiral simple diacetylenes have not been shown to be "nanoactive". Surprisingly, scanning electron microscopy showed that, with relatively simple processing, our synthetic product self-assembled into a remarkably monodisperse preparation of nanotubes in aqueous solution (Figure 2A). These monodisperse nanotubes were seen in the presence of amorphous material, but whenever a nanotube was formed, it was of a uniform diameter. Mass spectroscopy (see Supporting Information Figures S7 and S8) of the quaternization reaction product showed that a mixture of amine salts was present (10% **2**, 60% **3**, 30% **4**, and less than 1% **5**), raising the fascinating question of whether one of the compounds was exclusively responsible for tube formation or whether the tubes consisted of mixed populations of derivatized PDAs. We therefore synthesized each of the compounds as shown in Figure 1, method B, and processed each one individually. Only two of the compounds formed any structured material. The amine hydrobromide salt of compound **2** formed the cauliflower structures seen in Figure 2B, and compound **3** formed the nanotubes seen in Figure 2C. Compound **4** produced only amorphous material presumably because the headgroup is less hydrophilic. Interestingly, the quaternary ammonium salt (compound **5**) was in fact a liquid at room temperature, which explains its absence from the original nanotube-forming mixture. Carefully controlling the process conditions with compound **3** has allowed us to make preparations in which essentially 100% of the material self-assembles into nanotubes with identical diameters. Under the scanning electron microscope, the nanotubes are monodisperse with respect to wall thickness (27 nm) and internal diameter (35 nm) (Figure 2C). The tubes formed via methods A and B are identical in size. The precise structure of these remarkable "nanomacaroni" structures is revealed in the TEM and SAXS data reported below.

TEM observations of both naked nanotubes and nanotubes after staining with phosphotungstic acid reveal a hollow inner core and a wall consisting of five lipid bilayers (Figure 3A). The structure in solution was further characterized by SAXS. The results (Figure 3B) suggest that the equilibrium spacing of the tubule bilyaers in excess water is 57. 8 Å. Although the diameter of the tubes is uniform throughout the sample, the length varies, with a mean of approximately 1 μm.

As mentioned above, exposure to UV light induces a polymerization through the triple bonds of the diacetylene groups on adjacent molecules. This polymerization has been shown to be accompanied by a color change.[19] Nanotubes were dried onto glass surfaces and UV irradiated. This resulted in a

(19) Jonas, U.; Shah, K.; Norvez, S.; Charych, D. H. *J. Am. Chem. Soc.* **1999**, *121*, 4580−4588.

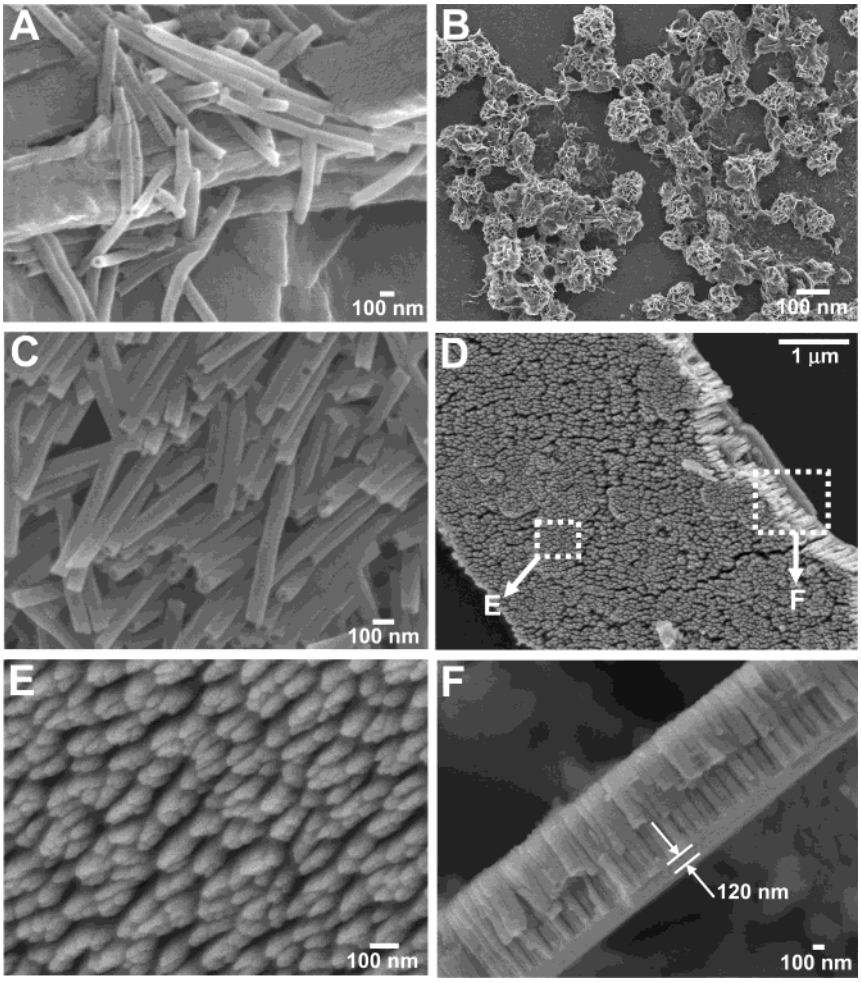

Figure 2. SEM images of the formation of nanotubes and nanocarpets: (A) nanotubes and lamellar structures formed from the intermediates of quaternization; (B) lamellar structures of the bromine salt of **2**; (C) linear nanotubes and one branched nanotube from compound **3** showing the monodispersity of the diameters; (D) nanocarpet; (E) front view of the nanocarpet; (F) side view of the nanocarpet.

color change from white to dark blue. Exposure of the polymerized nanotubes to detergents and strong acids induced a color change from blue to red or yellow (data not shown). Nanotubes recovered from the polymerization and examined by SEM were indistinguishable from non-cross-linked tubes (see Supporting Information Figure S9).

Nanocarpet Formation. One of the most striking results of our attempts to maximize the formation of nanotubes was the observation of the structure we term a nanocarpet (Figure 2D−F). Simple preparation of aligned surfaces of nanotubes and nanowires remains an elusive goal for many researchers. Such alignment is particularly important for applications such as colorimetric sensors and microelectronics.[20] The alignment of carbon nanotubes on silica-containing iron surfaces via thermal decomposition of acetylene gas in nitrogen gas has been reported[21] and is indicative of the fact that, in almost all reported cases, alignment of nanotubes requires a template. If the template is of monodisperse size distribution, aligned or ordered, so then are the nanotubes. Ordered nanotube arrays are then obtained upon removal of the template. Under certain conditions we have observed nanotubes clustering according to size (see Supporting Information Figure S10). We hypothesized that a mechanism which could allow such clusters to form would require significant nanotube-to-nanotube interaction. Using this mechanistic approach, we further hypothesized that if we could maximize inter-nanotube interactions during processing we may be able to align the tubes in a macrostructure. We prepared aqueous nanotubes and dried them onto a glass slide. Small droplets of chloroform were placed on the slide and allowed to evaporate. Material from the area around the chloroform droplets was scraped from the glass and observed by SEM. The results were unexpectedly compelling (Figure 2D).

We know that before exposure to chloroform the outer surface and inner surface of the nanotubes are hydrophilic and open-ended. Our current working hypothesis is that the addition of a small amount of chloroform to a disordered surface of nanotubes first melts the top surface of the tubes, creating a lamellar structure from which disoriented pillars can emerge (Figure 2E,F). It is, perhaps, the gradual removal of chloroform that then causes the tubes to become aligned. Whatever the mechanism, the pillars of the resulting nanocarpet are approximately 100 nm in diameter and 1 μm in length (Figure 2E,F). Each pillar consists of a cluster of 3−4 nanotubes of exactly the same diameter observed for the disordered nanotube systems described above. The carpet backing is 120 nm thick (Figure 2F).

(20) Okada, S.; Peng, S.; Spevak, W.; Charych, D. *Acc. Chem. Res.* **1998**, *31*, 229−239.
(21) Ren, Z. F.; Huang, Z. P.; Xu, J. W.; Wang, J. H.; Bush, P.; Siegal, M. P.; Provencio, P. N. *Science* **1998**, *282*, 1105−1107.

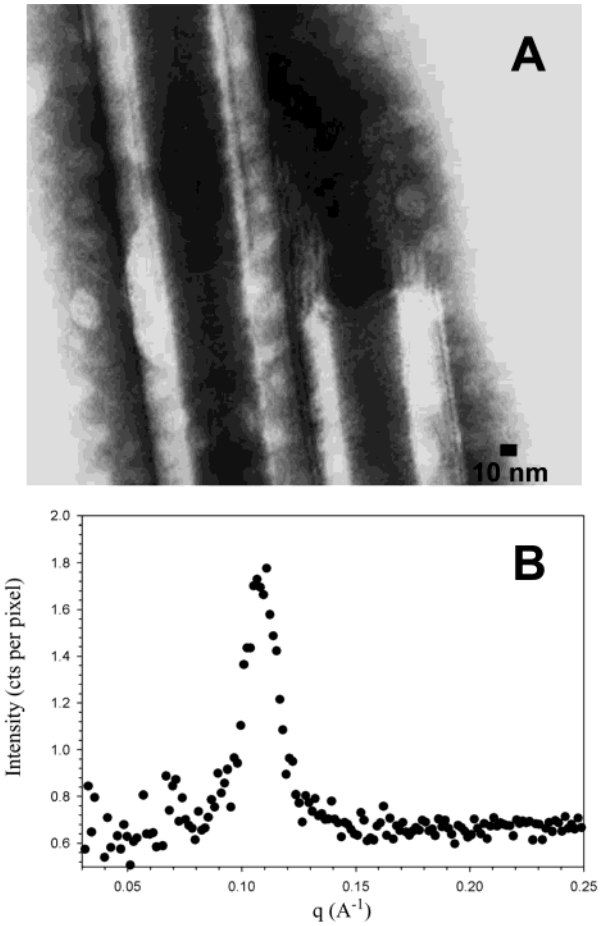

Figure 3. (A) TEM image of a nanotube showing the five-bilayer structures of the tubule walls. (B) SAXS of **3**.

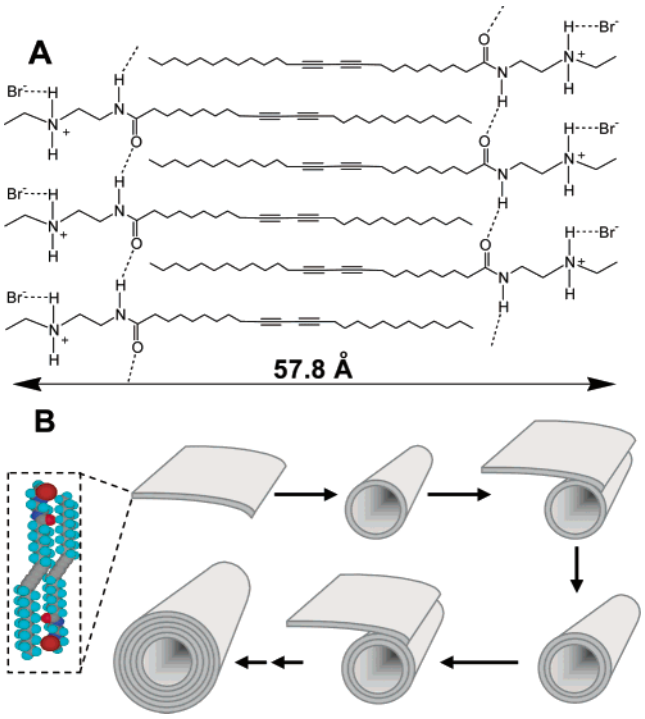

Figure 4. (A) Schematic structure of a bilayer of a nanotube. (B) Schematic of the assembly of a nanotube.

Table 1. Biocidal Activity of Nanotubes against *E. coli*

concn of nanotube material (μg/mL)	% kill, nonpolymerized nanotubes	% kill, polymerized nanotubes
10	100	100
5	100	100
1	99.2	26

Chirality. Recently, several studies have shown that molecular chirality may not be essential for formation of tubular structures by diacetylenic lipids.[7−9] In that vein, compound **3** has no discernible chiral center. However, a CD signal from **3** in water was observed, and the CD peak at 210 nm is enhanced in multilayer lamellar structures (see Supporting Information Figure S11). We presume that molecular chirality is induced *during* nanotube formation and perhaps drives the self-assembly. If the headgroup of compound **3** becomes chiral during self-assembly, the implication is that the amine inversion is prevented and each of the protons is in a nonexchangeable and different environment. One plausible explanation for the observation of a CD signal in **3** is that one proton is differentiated from the other by its interaction with the bromide ion. This would, in fact, create a chiral center. It is also possible that both protons interact with the bromide to form a ring structure that locks the nitrogen in a chiral configuration. It is interesting to note that, of all of the compounds in Figure 1, only compound **3** forms nanotubes and it is also the only one that can form a chiral center via differential counterion distribution. The precise nature of the chirality around the headgroup nitrogen will be explored in a specialized report on that topic. On the basis of all our data, we propose a schematic structure of the bilayers and their assembly into a nanotube (Figure 4). We hypothesize that the proton interacting with bromide is restricted and that the structure forms by intermolecular hydrogen-bonding of the amide hydrogen with an adjacent carbonyl oxygen and through hydrophobic interactions of the diacetylene tails. The number of bilayers in each tubule is presumably limited by the ability of a bilayer sheet to bend into a tubular shape with a five-bilayer structure as the most stable arrangement. Understanding how chirality forms from a simple achiral molecule will help us to understand the mechanism of tubule formation from many different complex lipid structures.

Antimicrobial Susceptibility Determination. Since our initial goal was to design molecules that both sensed and killed bacteria, several experiments were performed to assess the interaction of nanotubes with bacteria. The antimicrobial activity was tested by incubation of 3×10^5 *E. coli* cells in solutions containing 1, 5, and 10 μg/mL polymerized or nonpolymerized nanotubes. The results of these experiments are shown in Table 1. Treatment with 10 and 5 μg/mL concentrations of either polymerized or nonpolymerized nanotubes killed all of the cells within 1 h. When the concentration is reduced to 1 μg/mL, the number of surviving cells becomes measurable, with the nonpolymerized nanotubes killing more cells than an equivalent amount of polymerized tubes. The antimicrobial results were somewhat unexpected as antimicrobial activity is well-known in quaternary ammonium compounds but not as well described for secondary amine salts.

Response of Polymerized Nanotubes to Bacteria. When high concentrations of bacteria are mixed with high concentrations of polymerized nanotubes, the material acts as a flocculent, quickly causing the bacteria to settle out of solution. This activity is seen with bacterial concentrations of $>10^9$ cells/mL and nanotube concentrations of >50 μg/mL. When lower concentra-

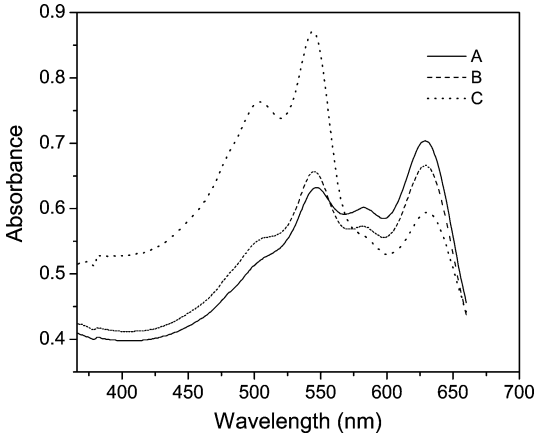

Figure 5. Optical detection of the interaction between *E. coli* and polymerized nanotubes: (A) nanotubes alone; (B) nanotubes plus 10^7 *E. coli* cells; (C) nanotubes plus 10^8 *E. coli* cells. The optical density of polymerized nanotubes with and without bacteria was scanned between 366 and 750 nm. The concentration of nanotubes was the same in all cases. The scans of nanotubes with bacteria were blanked with an equal concentration of bacteria in water.

tions of bacteria are used and the concentration of nanotubes is maintained at 50 μg/mL, a different pattern of behavior emerges. Mixing 1 mL of water containing $\sim 10^9$ bacterial cells with 1 mL of 100 μg/mL polymerized nanotubes caused an immediate color change from dark blue to red-pink, when the number of bacterial cells was reduced to 10^8, the color change took about 10 min, and when the number of bacterial cells was reduced to 10^7, no detectable change was seen over the course of 20 min. These observations were further investigated by scanning spectrophotometry. Comparison of wavelength scans of polymerized nanotubes alone with scans of polymerized nanotubes in the presence of 10^7 or 10^8 bacterial cells/mL (Figure 5) showed a progressive decrease in the absorbance peak at about 630 nm and an increase in the peaks at 540 and 500 nm. The nonpolymerized nanotubes do not show absorbance peaks in the visible range (data not shown). The change in the absorbance spectra seems to correspond to the ability to visually detect a color change. The color change also seems to be dependent on the ratio of cells to nanotubes, and this dependence will be the focus of future investigations. Additionally, it is unknown what the critical factor is in the color change. It is possible that the factor required is something released from the cells upon contact with the nanotubes. This question is currently under investigation.

Observation of Nanotube−Bacteria Interactions. A 1 mL sample of a solution of nonpolymerized nanotubes was prepared and mixed with 1 mL of a suspension which contained 10^9 *E. coli* cells. Nonpolymerized tubes were used in this experiment because, as stated above, the polymerized tubes clumped and precipitated with the cells, which would limit the ability to observe individual cells, a behavior not seen with nonpolymerized tubes. TEM grids were dipped in the mixture, excess liquid was wicked off, and the grids were observed with the transmission electron microscope. In these preparations the majority of the nanotubes were associated with the outer surface of the bacteria. Figure 6A shows a striking example of a nanotube that is fused with the outer surface of the bacterial cell, and

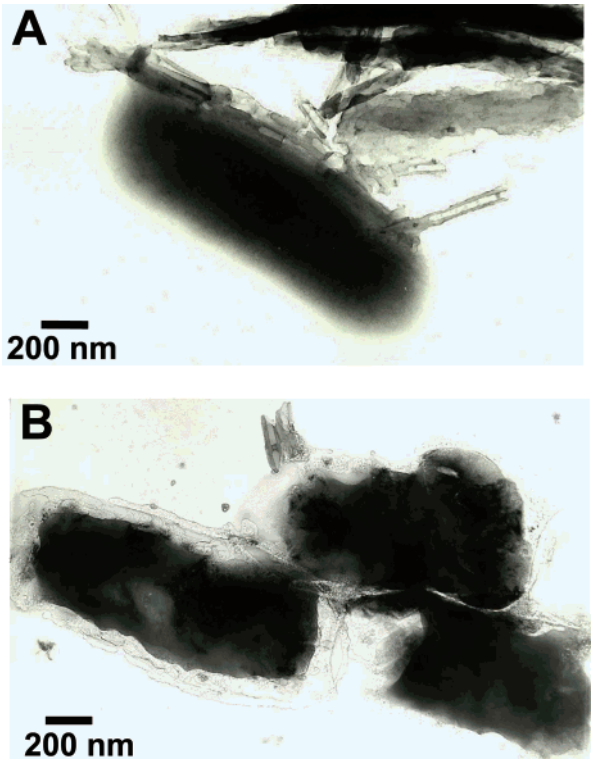

Figure 6. TEM images of nonpolymerized nanotubes mixed with *E. coli* cells.

Figure 6B shows a cell that has been completely enveloped by nanotubes. From these pictures it appears likely that the mechanism of kill does not involve a complete disruption of the cell wall of the bacteria as the rodlike structure of the *E. coli* cell is maintained.

In summary, the self-assembly of certain diacetylene amine salts under carefully controlled conditions induces the formation of an array of nanostructures. We have produced nanotubes with uniform diameters from a single starting material. Further processing can lead to the clustering of these materials by length and to the formation of what we term nanocarpets. Interest in the versatility of diacetylene amine salts as platform compounds for nanomaterial design and synthesis is enhanced by their biocidal nature and the ability of polymerized diacetylene amine salts to signal their interaction with cells.

Acknowledgment. This work was supported by the DoD Multidisciplinary University Research Initiative (MURI) (Grant DAAD19-01-1-0619) program administered by the Army Research Office. We also acknowledge An Ngo for the skilled preparation of samples for SAXS.

Supporting Information Available: Figures showing the mass spectrum of reaction products from Figure 1 (method A), mass spectrum of compound **3**, morphology of the nanotubes before and after polymerization by UV irradiation, SEM images of two groups of self-assembled nanotubes that formed clusters, and CD spectrum of an aqueous suspension of nanotubes made from compound **3** (PDF). This material is available free of charge via the Internet at http://pubs.acs.org.

JA048463I